

## pH-Dependent Assembly and Conversions of Six Cadmium(II)-Based Coordination Complexes

Hua-Cai Fang,<sup>†</sup> Ji-Qin Zhu,<sup>†</sup> Li-Jiang Zhou,<sup>‡</sup> Hong-Yang Jia,<sup>†</sup> Shan-Shan Li,<sup>†</sup> Xue Gong,<sup>†</sup> Shu-Bin Li,<sup>‡</sup> Yue-Peng Cai,<sup>\*,†</sup> Praveen K. Thallapally,<sup>\*,§</sup> Jun Liu,<sup>§</sup> and Gregory J. Exarhos<sup>§</sup>

<sup>†</sup>School of Chemistry and Environment, Key Laboratory of Electrochemical Technology on Energy Storage and Power Generation of Guangdong Higher Education Institutes, Engineering Research Center of Materials and Technology for Electrochemical Energy Storage (Ministry of Education), South China Normal University, Guangzhou 510006, China, <sup>‡</sup>College of Life Science, South China Normal University, Guangzhou 510631, China, and <sup>§</sup>Pacific Northwest National Laboratory, Energy and Environment Directorate, Richland, Washington 99352

Received April 6, 2010; Revised Manuscript Received May 6, 2010

**ABSTRACT:** Six cadmium(II) complexes containing the N<sub>2</sub>O<sub>2</sub> donor tetradentate unsymmetrical Schiff base ligand 2-[2-(dimethylamino)ethylimino]methyl]-6-methoxyphenol (HL<sup>5</sup>), namely, [(Cd<sub>3</sub>L<sup>5</sup>)<sub>2</sub>Cl<sub>2</sub>]·CH<sub>3</sub>OH·H<sub>2</sub>O (**1**), [Cd(L<sup>5</sup>)Cl]<sub>2</sub>·CH<sub>3</sub>OH (**2**), [Cd<sub>2</sub>(HL<sup>5</sup>)Cl<sub>4</sub>]<sub>n</sub> (**3**), {[Cd<sub>3</sub>(H<sub>2</sub>L<sup>5</sup>)<sub>2</sub>Cl<sub>8</sub>]·2H<sub>2</sub>O}<sub>n</sub> (**4**), [(H<sub>2</sub>L<sup>5</sup>)<sub>2</sub>]<sup>2+</sup>·[CdCl<sub>4</sub>]<sup>2-</sup>·H<sub>2</sub>O (**5**), and [(H<sub>2</sub>L<sup>5</sup>)<sub>2</sub>]<sup>2+</sup>·[CdCl<sub>4</sub>]<sup>2-</sup> (**6**), have been synthesized using cadmium(II) chloride and the unsymmetrical Schiff base ligand HL<sup>5</sup> under different pH conditions at room temperature. The diverse structures show the marked sensitivity of the structural chemistry of the tetradentate unsymmetrical Schiff base ligand HL<sup>5</sup>. Complex **1** formed at pH = 10 exhibits a rare zero-dimensional structure of trinuclear cadmium(II). At pH = 8–9, a dinuclear cadmium(II) complex **2** is formed. The reaction at pH = 5–7 leads to two one-dimensional structures of **3** and **4**. A further decrease of the pH to 3–5 results in a zero-dimensional structure **5**. Owing to the departure of lattice water molecules in the crystal, complex **5** at room temperature can gradually undergo single-crystal-to-single-crystal transformation to result in complex **6**. The results further show that conversions of complex **1–5** can also be achieved by adjusting the pH value of the reaction solution, **1**→**2**<sub>pH=8</sub>→**5**<sub>pH=3</sub> and **3**→**4**<sub>pH=5</sub>. Comparing these experimental results, it is clear that the pH plays a crucial role in the formation of the resulting structures, which simultaneously provides very effective strategies for constructing the Cd<sup>II</sup> compounds with N<sub>2</sub>O<sub>2</sub> donor tetradentate unsymmetrical Schiff base ligand. The strong fluorescent emissions of the six compounds (**1–6**) make them potentially useful photoactive materials. Furthermore, six Schiff base cadmium complexes (**1–6**), with 2,2-diphenyl-1-picrylhydrazyl (DPPH) as a co-oxidant exhibited the stronger scavenging activity.

### Introduction

In the past decade, good progress has been achieved in understanding the chemistry of transition metal complexes with unsymmetrical Schiff base ligands composed of primary amine and salicylaldehyde analogues.<sup>1</sup> Through different synthetic strategies metal complexes with intriguing topologies, biological activities as well as fluorescent properties have been successfully synthesized.<sup>2</sup> The Schiff base ligands containing imino (>C=N-), amino (-NR<sub>2</sub>), and hydroxyl (-OH) functionalities, self-assembled with various transition metal complexes are easily affected by physical and chemical stimuli.<sup>3,4</sup> In this regard, metal–organic frameworks constructed from rigid and flexible ligands have been shown to affect their structures by external stimuli such as temperature, pressure, and pH.<sup>4</sup> Understanding what causes these materials to respond to external stimuli can have applications in the development of smart materials.<sup>4,5</sup>

On the other hand, our research group has already reported some novel mono- and trinuclear Cd(II) complexes with the tripodal (HL<sup>1</sup>)/dipolar (HL<sup>2</sup>) imine-phenol Schiff base ligands through two different strategies of synthesis, that is, *template assembly* and *template destruction*.<sup>7</sup> Very recently, we have also prepared three tridentate/tetradentate unsymmetrical Schiff base ligands 2-[2-(dimethylamino)ethylimino]methylphenol (HL<sup>3</sup>, N<sub>2</sub>O donor set), methyl-2-pyridylmethylenedihydrazinecarbodi-

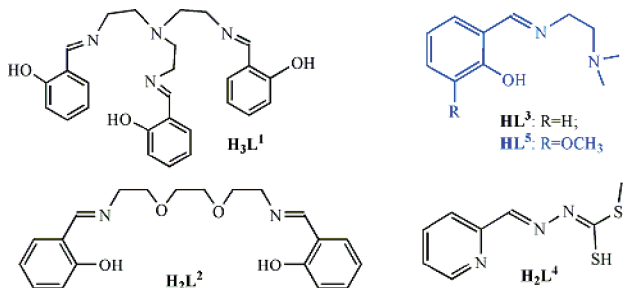
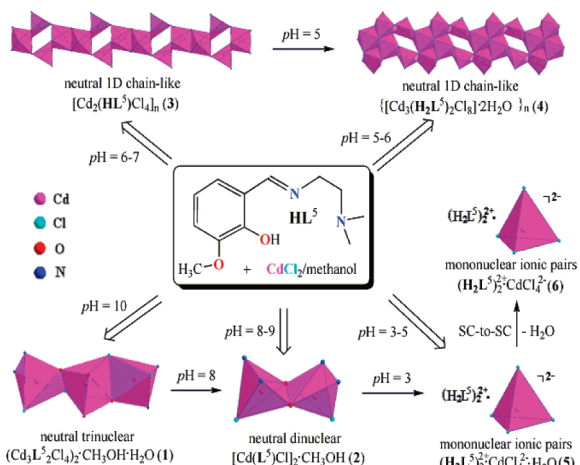
thioate (HL<sup>4</sup>, N<sub>2</sub>S donor set), and 2-[2-(dimethylamino)ethylimino]methyl-6-methoxyphenol (HL<sup>5</sup>, N<sub>2</sub>O<sub>2</sub> donor set) (Scheme 1), and a series of new cadmium complexes have been successfully synthesized and characterized.<sup>2d,8</sup>

As part of our ongoing study of metal complexes of the unsymmetrical Schiff bases, herein we report the self-assembly and conversion of six cadmium(II) complexes at different pH values. To understand the role pH played during self-assembly, we chose the unsymmetrical Schiff base HL<sup>5</sup> as an example directing the structure of the metal–organic complexes and supramolecular architectures. Herein we report the synthesis, crystal structures, and related properties of [(Cd<sub>3</sub>L<sup>5</sup>)<sub>2</sub>Cl<sub>2</sub>]·CH<sub>3</sub>OH·H<sub>2</sub>O, (**1**); Cd(L<sup>5</sup>)Cl]<sub>2</sub>·CH<sub>3</sub>OH (**2**); [Cd<sub>2</sub>(HL<sup>5</sup>)Cl<sub>4</sub>]<sub>n</sub> (**3**); {[Cd<sub>3</sub>(H<sub>2</sub>L<sup>5</sup>)<sub>2</sub>Cl<sub>8</sub>]·2H<sub>2</sub>O}<sub>n</sub> (**4**); [(H<sub>2</sub>L<sup>5</sup>)<sub>2</sub>]<sup>2+</sup>·[CdCl<sub>4</sub>]<sup>2-</sup>·H<sub>2</sub>O, (**5**); and [(H<sub>2</sub>L<sup>5</sup>)<sub>2</sub>]<sup>2+</sup>·[CdCl<sub>4</sub>]<sup>2-</sup> (**6**). The structures range from zero-dimensional (0D) mononuclear, dinuclear, and trinuclear complexes to a one-dimensional (1D) chain, fully revealing the pH effect on the assembly of metal organic complexes (Scheme 2). In contrast to the aforementioned cases containing unsymmetrical salen-type Schiff base ligands, fewer efforts have been devoted to the systematic investigation of Cd(II) coordination chemistry and the influence of reaction conditions.

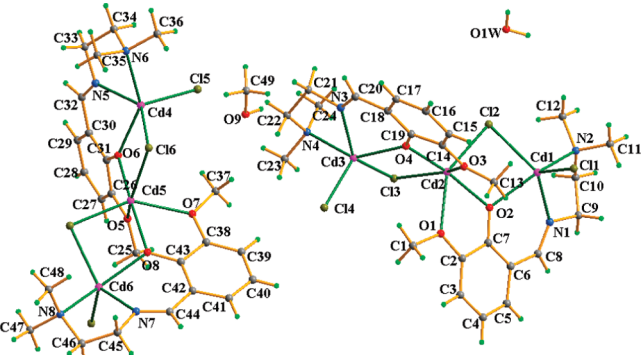
### Results and Discussion

**Preparation, Characterization, and Conversions.** The syntheses of six cadmium(II) Schiff base HL<sup>5</sup> complexes and their transformations are shown in Scheme 2, which illustrates the

\*To whom correspondence should be addressed. (Y.-P.C.) Fax: (+86) 20-39310187. E-mail: ypc18@yahoo.com. (P.K.T.) E-mail: Praveen.Thallapally@pnln.gov.

**Scheme 1. Several Salen-Type Schiff Base Ligands****Scheme 2. Syntheses and Conversion of Six Cadmium Complexes at Different pH Values**

sensitivity of the reaction conditions such as pH. It is noted that the same complex was obtained with the use of different molar ratios of cadmium(II) ions and ligand  $\text{HL}^5$  (1:1, 2:1, and 3:1, respectively) at a certain pH value. A methanolic solution containing cadmium chloride and organic ligand  $\text{HL}^5$  (3:1) will drive the reaction complete and lead to the isolation of cadmium(II)-organic complexes in high yield. When the reaction pH was maintained at 10, a trinuclear complex **1** was obtained as colorless platelike crystals in 75% yield. In contrast, when the reaction pH is between 8 and 9 and 3–5 a dinuclear compound **2** with 71% yield and mononuclear compound **5** with 82% yield resulted, respectively. Under different pH conditions such as 6–7 and 5–6, 1D chain-like complex **3** (yield 68%) and **4** (yield 78%) were respectively isolated. Meanwhile, the irreversible conversions also revealed their remarkable sensitivity to pH control: complex **1** transformed to complex **2** at pH = 8 and transformed to complex **5** at pH = 3. Furthermore, complex **3** was also converted to **4** at pH = 5. However, complex **6** was obtained by single-crystal-to-single-crystal conversion of **5** driven by the departure of the lattice water molecules at room temperature. These observations are a clear indication that the formation of six cadmium(II) Schiff base complexes are typically pH-dependent reaction patterns. In our case, all of the six complexes were isolated in pure single-crystal forms. X-ray diffraction studies showed that the hydroxyl group was deprotonated in **1–3**; however, the proton of the hydroxyl group in **3** was shifted to the amino group  $\{[-\text{NH}(\text{CH}_3)_2]^+\}$ , and ligand  $\text{HL}^5$  in the present case remained neutral. Because of high acidity, the ligand  $\text{HL}^5$  in **4**, **5**, and **6** was further protonated into  $(\text{H}_2\text{L}^5)^+$ , resulting in the loss of the coordinating ability of the oxygen and nitrogen atoms.

**Figure 1.** Molecular structure of trinuclear complex **1** with the atom-numbering scheme.

The IR spectra of four complexes (**1–4**) show that a small red shift appears in  $\nu(\text{C}-\text{O})$  compared with the free  $\text{HL}^5$  values, indicating that the hydroxyl O atom of ligand  $\text{HL}^5$  connected to central metal Cd<sup>II</sup> ions. In addition, we observed the very wide bands for  $\nu(\text{O}-\text{H})$  at 3405 to 3548 cm<sup>-1</sup> for  $\text{HL}^5$  and complexes **5** and **6** as compared to their disappearance in **1–4**. These results coincide with the analytical results of the single-crystal structures of  $[(\text{Cd}_3\text{L}^5_2\text{Cl}_4)_2]\cdot\text{CH}_3\text{OH}\cdot\text{H}_2\text{O}$  (**1**),  $[\text{Cd}(\text{L}^5)\text{Cl}]_2\cdot\text{CH}_3\text{OH}$  (**2**),  $[\text{Cd}_2(\text{HL}^5)\text{Cl}_4]_n$  (**3**),  $\{[\text{Cd}_3(\text{H}_2\text{L}^5)_2\text{Cl}_8]\cdot 2\text{H}_2\text{O}\}_n$  (**4**),  $[(\text{H}_2\text{L}^5)_2]^{2+}\cdot[\text{CdCl}_4]^{2-}\cdot\text{H}_2\text{O}$  (**5**), and  $[(\text{H}_2\text{L}^5)_2]^{2+}\cdot[\text{CdCl}_4]^{2-}$  (**6**). The C=N peak of the ligand at 1632 cm<sup>-1</sup> is respectively red-shifted to 1615, 1610, and 1607 cm<sup>-1</sup> in complexes **1–3**, indicating the complexation of the imine nitrogen with the metal center.

To examine the thermal stability of the complexes, the thermogravimetric (TG) analyses of six compounds (**1–6**) were carried out from 20 to 800 °C. Thermal analysis of complex **1** shows a 20% weight loss between room temperature to 450 °C in three steps. The first weight loss between 75 to 150 °C corresponds to the loss of one water and methanol molecules (calcd. 2.73%, found 2.69%) followed by a decomposition of the sample at 450 °C. The TG curve of **2** indicates the loss of one molecule of methanol between 70 to 150 °C (calcd. 4.15%, found 4.12%) with simultaneous decomposition beyond 300 °C, while the preliminary TG analysis of  $\{[\text{Cd}_3(\text{H}_2\text{L}^5)_2\text{Cl}_8]\cdot 2\text{H}_2\text{O}\}_n$  (**4**) and  $[(\text{H}_2\text{L}^5)_2]^{2+}\cdot[\text{CdCl}_4]^{2-}\cdot\text{H}_2\text{O}$  (**5**) shows the loss of two water molecules for **4** (calcd. 4.26%, found 4.31%) and one water molecule for **5** (calcd. 5.01%, found 5.12%), respectively. Finally, both the coordination frameworks decompose at high temperatures. As for complexes **3** and **6**, their preliminary TG analyses show no weight loss below 200 °C, and the coordination framework decomposes at 300 °C for **3** and 200 °C for **6** (Supporting Information, Figure S1).

**Crystal Structures of Six Compounds.** Single-crystal structural analysis of  $[(\text{Cd}_3\text{L}^5_2\text{Cl}_4)_2]\cdot\text{CH}_3\text{OH}\cdot\text{H}_2\text{O}$  (**1**) shows the neutral tricadmium complex consists of two trinuclear units of  $\text{Cd}_3\text{L}^5_2\text{Cl}_4$ , one methanol, and water molecule as shown in Figure 1. Each trinuclear  $\text{Cd}_3\text{L}^5_2\text{Cl}_4$  unit contains three independent Cd(II) centers with two different coordination geometries. Out of two cadmiums (Cd1, Cd3, Cd4, Cd6) one is five-coordinated by two amino nitrogen atoms and one hydroxyl oxygen atom from one  $\text{HL}^5$  and two chloride atoms (one  $\mu^2$ -bridging Cl and the other terminal Cl) with an average Cd–N bond distance of 2.313(6) Å, a Cd–Cl bond distance of 2.488(2) Å, and a Cd–O bond distance of 2.255(4) Å. The bond angles around Cd1 (Cd3, Cd4, Cd6) are in the range of 76.4(2) to 145.1(2)°. The coordination geometry around a Cd1 (Cd3, Cd4, Cd6) atom is a distorted

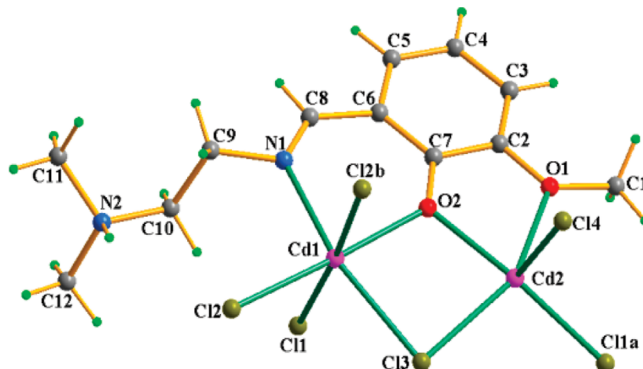


**Figure 2.** Perspective view of the coordination environments of the metal atoms in the asymmetric unit of compound 3.

square pyramid. On the other hand, the second cadmium (Cd2, Cd5) is six-coordinated by four oxygen atoms from two different  $\text{HL}^5$  ligands and two  $\mu^2$ -bridging chloride atoms with a distorted octahedral geometry. The average Cd–O distance around Cd2 (Cd5) is 2.323(4) Å, and the Cd–Cl distance is 2.5840(17) Å. The bond angles around Cd2 (Cd5) range from 107.76(6) to 109.71(6)°. Moreover, each trinuclear cadmium motif as a building block is assembled into a dimer between the same two units, through weak hydrogen bonds C–H $\cdots$ Cl ( $\text{H}\cdots\text{Cl}$  2.728 Å,  $\angle \text{CHCl}$  = 156.9(5)°, the symmetrical code a: 1 –  $x$ , – $y$ , 1 –  $z$ )/C–H $\cdots$ Cl ( $\text{H}\cdots\text{Cl}$  2.803 Å,  $\angle \text{CHCl}$  = 153.1(5)°, and the symmetrical code a: – $x$ , 1 –  $y$ , 2 –  $z$ ) (Figure S2, Supporting Information).<sup>9</sup>

When the reaction solution of  $\text{HL}^5$  and  $\text{CdCl}_2$  was adjusted to pH = 8–9, complex **2**,  $[\text{Cd}(\text{L}^5)\text{Cl}]_2 \cdot \text{CH}_3\text{OH}$ , was isolated as colorless block crystals, which was recently reported by us.<sup>6</sup> As shown in Figure S3, Supporting Information, due to the alkaline environment, the Schiff base in complex **2** still presents the deprotonated form ( $\text{L}^5^-$  like complex **1**).

Unlike complex **1**, it is interesting to note that the uncoordinated solvent methanol molecules in **2** each form 1D methanol chains via strong O–H $\cdots$ O hydrogen bonding interactions with helical characters that adopt the alternate arrangement of  $\Delta$ - and  $\Lambda$ -helical chains (Figure S4, Supporting Information).

When the pH of the reaction solution was further reduced to 6–7, complex **3** was obtained as pale yellow crystals, and the crystallographic analysis confirmed that the hydroxyl proton of the  $\text{HL}^5$  ligand was shifted into the amino group in the neutral ligand  $\text{HL}^5$ , and as a result, each  $\text{HL}^5$  in **3** acts as a tridentate  $\text{NO}_2^-$  donor set to coordinate with two cadmium atoms. As shown in Figure 2, there are two different Cd(II) centers and one independent  $\text{HL}^5$  ligand in the asymmetric unit of **3**. The Cd1 is six-coordinated by one oxygen and one nitrogen atom from one ligand  $\text{HL}^5$  as well as four chloride atoms to present a distorted octahedral geometry with an average Cd1–Cl separation of 2.645(2) Å. However, the Cd2 atom is five-coordinated by two oxygen atoms from one  $\text{HL}^5$  and three chloride atoms, and the coordination geometry around Cd2 is a distorted square pyramid with an average Cd2–Cl distance of 2.498(2) Å. On the other hand, all three chloride atoms—Cl1, Cl2, and Cl3  $\mu^2$ -bridge to two cadmium ions to generate a zigzag chain structure (Figure 3). The 1D chains are further connected via  $\pi\cdots\pi$  interactions with the centroid-to-centroid distance of 3.825 Å between two benzene rings from two adjacent chains to form a 2D layer-like structure along the  $c$  axis (Figure 4). In addition, the presence of interlayer hydrogen bonds (C–H $\cdots$ Cl) leads

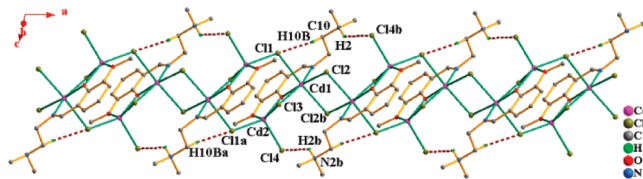


**Figure 3.** View of a 1D zigzag chain structure of **3** linked by three  $\mu^2\text{-Cl}$  bridges with hydrogen bonds C–H $\cdots$ Cl and N–H $\cdots$ Cl indicated by dashed lines. Symmetrical code a: – $x$ , 2 –  $y$ , 2 –  $z$ ; b: 1 –  $x$ , 2 –  $y$ , 2 –  $z$ .

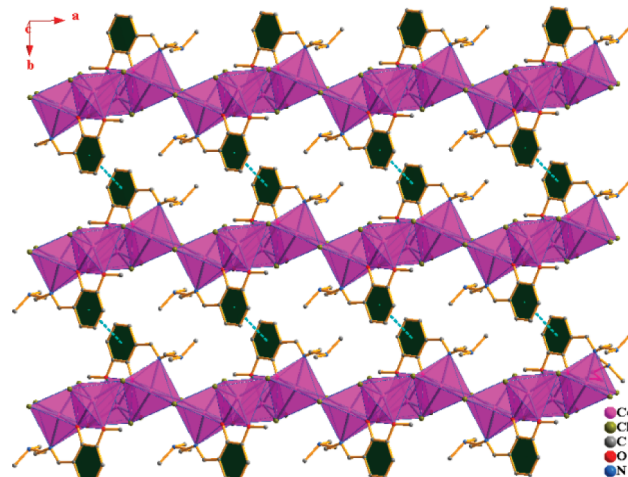


**Figure 4.** 2D sheet in **3** constructed by  $\pi\cdots\pi$  stacking between the two adjacent 1D chains in the  $ab$  plane. H atoms were omitted for clarity.

to the formation of a 3D supramolecular network (Figure S5 and Table S1), which contributes to the additional stability of the structure.<sup>10</sup>

As the pH of the reaction solution was adjusted to ca. 5–6, complex **4** was generated. It is interesting to find that both amino and imino groups of the  $\text{HL}^5$  ligand in **4** are protonated in the form of  $(\text{H}_2\text{L}^5)^+$ . In the present case, each protonated  $(\text{H}_2\text{L}^5)^+$  ligand only acts as a bidentate  $\text{O}_2$  donor to chelate one cadmium atom. From Figure 5, it is clear that there are three different Cd(II) centers, six  $\mu^2\text{-Cl}$  atoms, one terminal Cl atom, and one independent ligand in the asymmetric unit. All three Cd(II) atoms are six-coordinated with the same coordination geometries of distorted octahedrons, but the coordination environment of Cd1 and Cd2(Cd3) is different. The Cd1 is connected to two  $\mu^2\text{-Cl}$ , two  $\mu^3\text{-Cl}$ , and two chelated O atoms from the same ligand with average bond distances of Cd–Cl 2.618 Å and Cd–O 2.343(2) Å. The second Cd2 (Cd3) is connected to one terminal Cl, two  $\mu^2\text{-Cl}$ , and three  $\mu^3\text{-Cl}$  atoms with average bond distances of Cd–Cl 2.659(1) Å for Cd2 and 2.640(1) Å for Cd3.

The single crystal X-ray analysis shows that complex **4** presents a 1D chain-like structure along the  $a$ -axis (Figure 6). It is noteworthy that compound **4** possesses a 1D chain-like core  $[\text{Cd}_3(\mu^2\text{-Cl})_3(\mu^3\text{-Cl})_3]_n$ .

Close scrutiny of complex **4** shows the 2D supramolecular layer consist of strong and weak O–H $\cdots$ O and O–H $\cdots$ Cl hydrogen bonds originated from noncoordinated water molecule and a coordinated chloride ion (Table S1) (Figure 7). Moreover, each 2D layer interacts with two neighboring ones, each via edge-to-face C–H $\cdots$  $\pi$  interactions (Table S1), forming extended 3D supramolecular network structures (Figure S6). This contributes to the additional stability of the structure.<sup>7</sup>

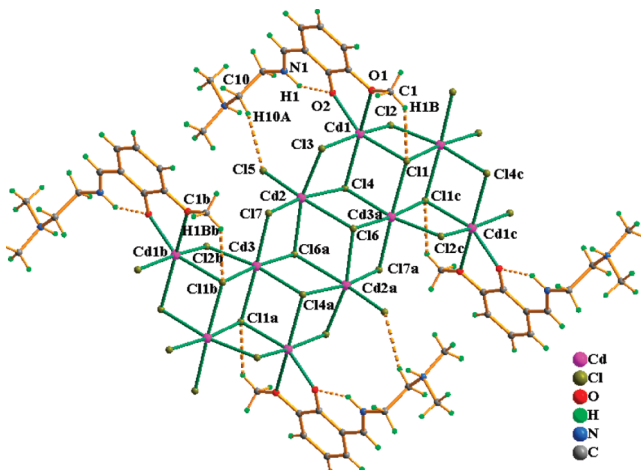


**Figure 5.** Coordination environment of three different cadmium ions in the unsymmetrical unit of **4**. Uncoordinated water molecules were omitted for clarity. The dashed lines denote the intrachain hydrogen bonds.

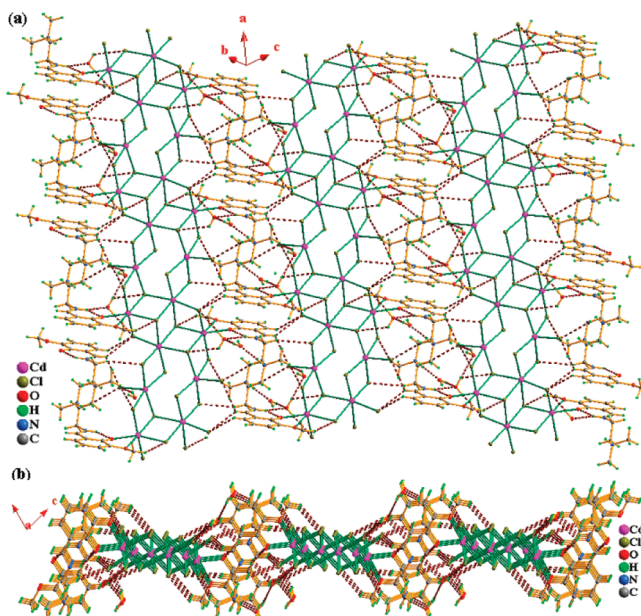


**Figure 6.** One-dimensional chain with the alternate arrangement of the reversely oriented face-sharing defect cubanes extending along the *a* axis in **4**.

To further investigate the influence of pH on the formation and structure of the complexes, the pH of the reaction solution was adjusted to 3–5, and the orange complex **5** was generated. The crystallographic analysis revealed that the structure of **5** consists of one protonated  $[H(HL)]_2^{2+}$  cation, one  $[CdCl_4]^{2-}$  anion, and one water molecule in one asymmetrical unit as shown in Figure 8. It is reasonable that the ligand did not coordinate with the Cd(II) atom under the experimental conditions since the amino group in the ligand is protonated. Simultaneously, the hydroxyl group has not been deprotonated, thus losing the capability to coordinate with the metal atom. Therefore, two protonated ligands are dimerized to a cationic  $[H(HL^5)]_2^{2+}$  motif by hydrogen bonds  $N-H\cdots O$ ,  $O-H\cdots N$ , and  $\pi\cdots\pi$  stackings between two benzene rings (Figure 8 and Table S1). On the other hand, the Cd(II) in each anion unit is coordinated by four chloride ions

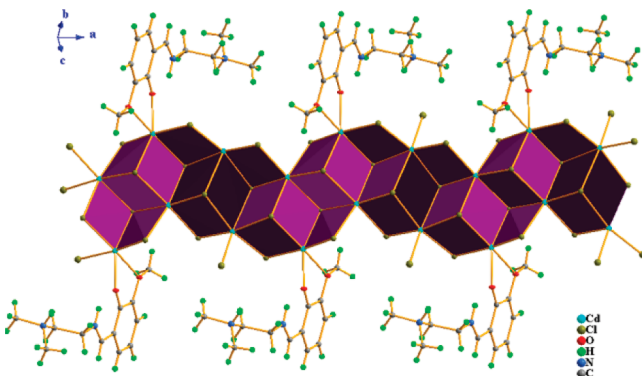


**Figure 7.** 2D sheet in **4** constructed by  $O-H\cdots O$  and  $O-H\cdots Cl$  and  $C-H\cdots\pi$  stacking interactions between the two adjacent 1D chains.

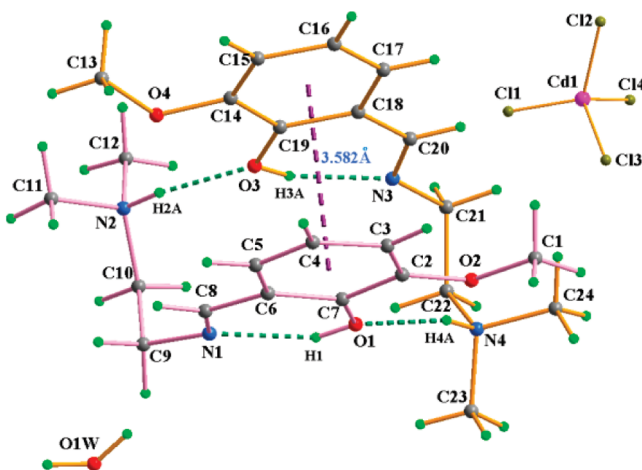


**Figure 8.** View drawing of **5** with hydrogen bonds  $N-H\cdots O$  (green) and  $\pi\cdots\pi$  stacking (pink) between two benzene rings indicated by dashed lines.

to form a  $[CdCl_4]^{2-}$  unit with distorted tetrahedral geometry. The Cd–Cl bond distances are from 2.439(4) to 2.483(4) Å, and the Cl–Cd–Cl angles fall in the range of 106.86(13)° and 111.28(15)° (Table S2), which are similar to those reported.<sup>12</sup> Moreover, the anionic  $[CdCl_4]^{2-}$  units and the protonated  $[H(HL^5)]_2^{2+}$  cation units are further joined together through  $C-H\cdots Cl$  hydrogen bonds (Table S1) to form a three-dimensional (3D) structure (Figure S7).

When exposed in the air for about 3 days, the orange crystals of **5** gradually became pale yellow. The X-ray structure determination on pale yellow crystals revealed that complex **5** undergoes single-crystal to single-crystal transformation to **6** with the loss of one water molecule. The structure of the crystal **6** is very similar to that of **5** as shown in Figure 9. The difference is only that there are no lattice water molecules in compound **6** derived from the departure of water molecules during the single-crystal-to-single-crystal transformation of **5**. Similar to compound **5**, the 3D supramolecular network in **6** is also constructed by strong and weak hydrogen bonds ( $N-H\cdots O$ ,  $O-H\cdots N$ , and  $C-H\cdots Cl$ ) (Figure S8 and Table S1).

As discussed above, complexes **1–6** are obtained from the same reactants and the reaction conditions but with a slight change in the pH values, respectively. This is based on the ligand  $HL^5$  potentially assuming abilities of both donor and acceptor for hydrogen, through the tuning of the reaction

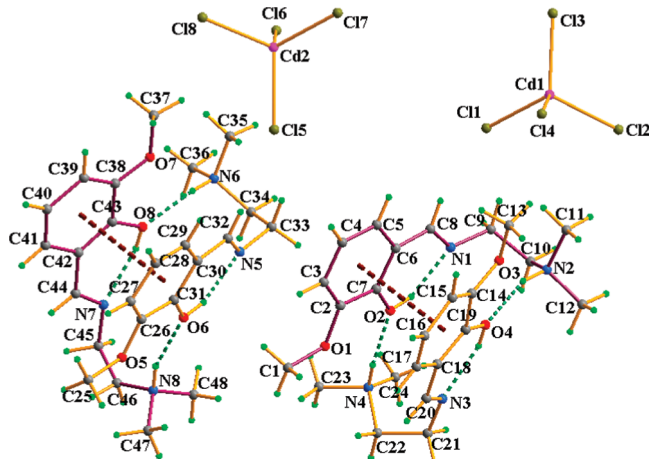


**Figure 9.** Molecular structure of compound **6** with the atom-numbering scheme. The dashed lines denote the intermolecular hydrogen bonds (green)  $\text{N}-\text{H}\cdots\text{O}$ ,  $\text{O}-\text{H}\cdots\text{N}$ ,  $\text{C}-\text{H}\cdots\text{Cl}$ , and  $\pi\cdots\pi$  stackings (brown).

pH. To further explore the influence of pH values on six resulting Cd-complexes, the interconversions among these complexes were also carried out. The results show that on decreasing pH, compound **1** may convert to **2** at a pH ca. 8 and **2** to **5** at a pH ca. 3. Compound **3** may also convert to **4** at a pH ca. 5. At the same time, the related experiments further confirmed that these transformations are irreversible (Scheme 2).

**Photophysical Properties.** Considering that compounds **5** and **6** have the same structures in the solution, the fluorescence properties of the Schiff base ligand ( $\text{HL}^5$ ) and their Cd(II) complexes **1–5** were studied at room temperature (298 K) in methanol solution ( $10^{-5}$  mol/L, Figure 10). The emission spectra of complexes **1–5** resemble that of the ligand  $\text{HL}^5$ , excluding the emission intensity. This indicates that the fluorescence of these complexes is from L-based emission. The green emission for complexes **1–5** and  $\text{HL}^5$  can be observed where the maximum emission wavelength is at 476 nm (under 369-nm excitation) for the ligand  $\text{HL}^5$ , and 470, 471, 471, 472, and 474 nm (under 371-nm excitation) for complexes **1–5**, respectively. The lifetimes of compounds **1–5** are about 19.8, 18.5, 15.3, 15.1, and 8.2 ns, respectively, which are similar to other Cd-organic complexes.<sup>11</sup> Compared with the emission spectra of the ligand  $\text{HL}^5$ , slightly blue shifts of 6 nm, 5 nm, 5 nm, 4 nm, and 2 nm for **1–5** have been respectively given, which are considered to mainly arise from the coordination of donor atoms to the Cd(II) center. This hinders further interactions of the protonic solvent molecules. As a result, the  $\pi-\pi^*$  energy barrier of free ligand  $\text{HL}^5$  is slightly lower than the ligands in complexes **1–5**, resulting in slight blue-shift emission spectra of **1–5** compared with the free ligand.<sup>13</sup> Moreover, incorporating Cd(II) effectively increases the conformational rigidity of the ligand in compounds and reduces the loss of energy via vibration motions. Even complex **5**, where  $\text{HL}^5$  is not directly coordinated to Cd atoms, shows a slight increase in the fluorescence intensity as compared to the free ligand. This is because the anionic  $[\text{CdCl}_4]^{2-}$  units and the protonated  $[\text{H}(\text{HL}^5)]_2^{2+}$  cation units are joined together through  $\text{C}-\text{H}\cdots\text{Cl}$  hydrogen bonds to form a more rigid 3D structure.<sup>14</sup> Thus, the enhanced fluorescence intensities of the five complexes are detected, which open up the opportunity for photochemical applications of these complexes.<sup>15</sup> The intensive and

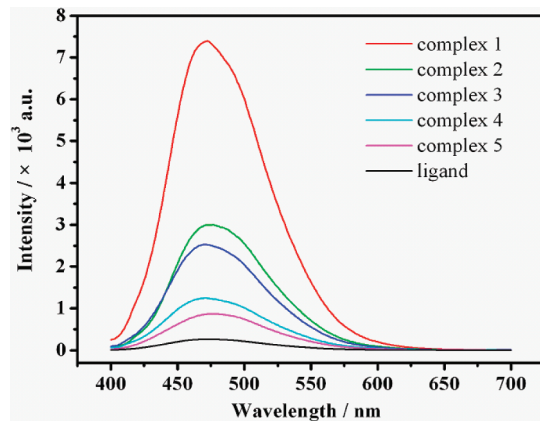


**Figure 10.** The emission spectra for complexes **1–5** and organic building block.

tunable fluorescence emissions of five complexes make them potentially useful photoactive materials in photophysical chemistry.

To further understand the fluorescent properties, the fluorescence quantum yields and lifetime of complexes **1–5** and ligand  $\text{HL}^5$  were investigated. From Table S2, it can be seen that the quantum yields are higher and the fluorescence lifetimes are longer for complexes **1** to **5** compared with the ligand  $\text{HL}^5$ , which is also derived from the big conformational rigidity of complexes **1–5**.<sup>11</sup> It is important to note the similarity in the photophysical properties between the free ligand and complex **5**, particularly the fluorescence quantum yield, the optical density, and the fluorescence lifetime (Table S2). This results from the absence of coordination of Cd atoms with the Schiff base ligand, resulting in poor restraint of solvent-ligand interactions and a similar  $\pi-\pi^*$  energy barrier to the ligand.

**DPPH Radical Scavenging Activity.** The DPPH assay was used to evaluate the capability of antioxidants to quench the stable DPPH radical. Antioxidant converts DPPH to 2,2-diphenyl-1-picryl hydrazine. This assay provides stoichiometric information with respect to the number of electrons taken up by the tested compounds in the presence of a stable radical. It is a very sensitive, and rapid method, which was very convenient for the screening of many samples of different polarity. Hence, in the present case, the potential antioxidant capability of methanol extracts containing compounds with different concentrations was evaluated by the DPPH (Figure S10). The free-radical scavenging activity is translated into IC<sub>50</sub> (inhibitory concentration to inhibit 50% of FRS activity), and a stronger radical-quenching agent resulted in a lower IC<sub>50</sub> value. It is clearly shown that the average radical scavenging activity of complex **5** (IC<sub>50</sub> = 0.125 mg/mL) for DPPH is the highest of all compounds and increases with the increase of the concentration (Figure S10 and Table S3). Compound **2** (IC<sub>50</sub> = 0.143 mg/mL) is the poorest effective inhibitor. However, complex **3** shows the largest FRS activity among all the other complexes and at all concentrations. With the increase of concentration, in particular, in the range of 0.03–0.1 mg/mL, the scavenging activity is rapidly enhanced. This is particularly the case with the FRS activity of complex **5**. Compared with standard samples of VC and BHT, IC<sub>50</sub> values of 0.114 mg/mL and 0.436 mg/mL, respectively, compounds **3** and **5** are obviously very good candidates as antioxidants. At present, the systematic research for those biological activities is in progress.

## Conclusions

In conclusion, six cadmium(II) complexes containing  $\text{N}_2\text{O}_2$  donor tetradentate asymmetrical Schiff base ligands have been synthesized at room temperature and structurally characterized. Compounds **1** and **2** obtained at alkaline condition exhibit 0D polynuclear Cd-structures with the deprotonated tetradentate Schiff base ligand ( $\text{L}^5^-$ ). Compounds **3** and **4** obtained at a slightly acidic environment have 1D chain-like structures with the neutral tridentate Schiff base ligand ( $\text{HL}^5$ ) and the protonated bidentate Schiff base ligand ( $\text{H}_2\text{L}^5^-$ ), respectively. Compound **5**, obtained at a strong acidic condition, shows a 0D ion-pair structure with the protonated Schiff base ligand ( $\text{H}_2\text{L}^5^-$ ) free coordinating to the Cd(II) ion. Meanwhile, further investigations show that on decreasing pH, some of compounds (**1–5**) may be irreversibly converted, that is, **1** → **2** → **5**, and **3** → **4**. However, compound **6** came from the conversion of single-crystal to single-crystal of **5** at room temperature. Clearly, in the present system, the pH of the reaction solution is responsible for the formation of these compounds with different topologies. Meanwhile, these synthetic strategies also provide the very effective means for constructing Cd<sup>II</sup> compounds with  $\text{N}_2\text{O}_2$  donor tetradentate asymmetrical Schiff base ligands. The strong fluorescence emissions of **1–5** make them potentially useful photoactive materials. In addition, the scavenging activities of compounds **1–5** on the DPPH are more effective than that of the ligand, in which compounds **3** and **5** are the most effective. It is clear that the scavenging activity on the DPPH can be enhanced by the formation of metal–ligand coordination complexes.

## Experimental Section

**Physical Methods.** All materials were reagent grade, obtained from commercial sources, and used without further purification; solvents were dried by standard procedures. Ligand  $\text{HL}^5$  (complexes) was prepared according to the reported procedure.<sup>16</sup> Elemental analyses for C, H, and N were performed on a Perkin-Elmer 240C analytical instrument. IR spectra were recorded on a Nicolet FT-IR-170SX spectrophotometer in KBr pellets. The mass spectra (FAB-MS) were recorded on a ZAB-HS spectrometer. The luminescent spectra for the solid state were recorded at room temperature on Hitachi F-2500 and Edinburgh-FLS-920 with a xenon arc lamp as the light source. In the measurements of emission and excitation spectroscopy, the pass width is 5.0 nm. Thermal analyses (under oxygenated atmosphere, heating rate of 5 °C/min) were carried out in a Labsys NETZSCH TG 209 Setaram apparatus. The antioxidative activity was performed in methanol with a 72 spectrophotometer.

**Preparation of Compounds **1–5**.** A methanol solution (4 mL) of  $\text{CdCl}_2$  (0.60 mmol) was mixed under stirring with the solution (6 mL) of the ligand  $\text{HL}^5$  (0.20 mmol) in the same solvent at room temperature under different pH value conditions (pH values were adjusted by adding an appropriate amount of triethylamine or dilute hydrochloric acid, and shown by pH meter). After the mixture was continuously stirred for 2 h and filtrated, the resulting clear solution was allowed to evaporate slowly at room temperature for one week, yielding testable crystals, which were collected by filtration, washed with methanol and ether successively, and dried in air. The pH value and characterization data for each compound are given below.

**Characterization Data of  $[(\text{Cd}_3\text{L}^5_2\text{Cl}_4)_2 \cdot \text{CH}_3\text{OH} \cdot \text{H}_2\text{O}]$  (1).** pH = 10. Yield 75% (based on the Cd). Elemental analysis calcd (%) for  $\text{C}_{49}\text{H}_{74}\text{Cl}_8\text{N}_8\text{O}_{10}\text{Cd}_6$ : C, 31.06; H, 3.91; N, 5.92. Found: C, 31.01; H, 4.06; N, 5.98. Fourier transform infrared (FT-IR) (KBr,  $\text{cm}^{-1}$ ): 3493 (br, w), 2889 (br, w), 2841(w), 1635(vs), 1615(m), 1557(w), 1457(vs), 1443(vs), 1399 (m), 1297(s), 1242(s), 1216(vs), 1080(m), 1020(m), 932 (m), 850 (m), 777(m), 743(m), 633(w), and 563 (w). Fast atom bombardment mass spectroscopy (FAB-MS):  $m/z$  922 ( $[(\text{Cd}_3\text{L}^5_2\text{Cl}_4) + 1]^+$ , 48%), 921 ( $[(\text{Cd}_3\text{L}^5_2\text{Cl}_4)^+]$ , 75%).

**Characterization Data of  $[\text{Cd}(\text{L}^5)\text{Cl}_2 \cdot \text{CH}_3\text{OH}]$  (2).** pH = 8–9. Yield 71% (based on the Cd). Elemental analysis calcd (%) for  $\text{C}_{25}\text{H}_{38}\text{Cl}_2\text{N}_4\text{O}_5\text{Cd}_2$ : C, 38.95; H, 4.93; N, 7.27. Found: C, 38.91; H, 5.01; N, 9.25. FT-IR (KBr,  $\text{cm}^{-1}$ ): 3494–3692(br., w), 2958(m), 2980(m), 2841(m), 1637(vs), 1610(m), 1599(s), 1467(s), 1448(s), 1396(m), 1375(w), 1337(w), 1298(s), 1236(s), 1217(vs), 1082(s), 967(m), 936(m), 886(m), 848(m), 783(m), 744(s), 732(s), 629(w), 561(w), 476(w). FAB-MS:  $m/z$  720 ( $[\text{M}]^+ - \text{CH}_3\text{OH}$ , 63%).

**Characterization Data of  $[\text{Cd}_2(\text{HL}^5)\text{Cl}_4]_n$  (3).** pH = 6–7. Yield 68% (based on the Cd). Elemental analysis calcd (%) for  $\text{C}_{12}\text{H}_{18}\text{Cl}_4\text{N}_2\text{O}_2\text{Cd}_2$ : C, 24.45; H, 3.06; N, 4.75. Found: C, 24.39; H, 2.98; N, 4.79. FT-IR (KBr,  $\text{cm}^{-1}$ ): 3493(br, m), 2841(w), 1635(vs), 1607(s), 1557(m), 1456(vs), 1443(vs), 1399(s), 1297(s), 1242(m), 1216(vs), 1101(w), 1080 (m), 1020(m), 964(w), 932(m), 850(m), 777(s), 743(s), 633(m), 563 (w). FAB-MS:  $m/z$  589 ( $[\text{M}]^+, 67\%$ ).

**Characterization Data of  $[(\text{Cd}_3(\text{H}_2\text{L}^5)_2\text{Cl}_8) \cdot 2\text{H}_2\text{O}]$  (4).** pH = 5–6. Yield 78% (based on the Cd). Elemental analysis calcd (%) for  $\text{C}_{12}\text{H}_{23}\text{Cl}_8\text{N}_2\text{O}_4\text{Cd}_3$ : C, 17.05; H, 2.72; N, 3.31. Found: C, 16.97; H, 2.76; N, 3.42. FT-IR (KBr,  $\text{cm}^{-1}$ ): 3569(br, m), 2986(w), 2727(w), 1632(vs), 1549(m), 1495(s), 1457(vs), 1372(w), 1339(w), 1297(m), 1227-vs), 1162(m), 1081(s), 1028 (m), 954(m), 850(w), 785(m), 752(m), 733(m), 633 (w). FAB-MS:  $m/z$  808 ( $[\text{M}]^+ - 2\text{H}_2\text{O}$ , 79%).

**Characterization Data of  $[(\text{H}_2\text{L}^5)_2]^{2+} \cdot [\text{CdCl}_4]^{2-} \cdot \text{H}_2\text{O}$  (5).** pH = 3–5. Yield 82% (based on Cd). Elemental analysis calcd (%) for  $\text{C}_{24}\text{H}_{40}\text{Cl}_4\text{N}_4\text{O}_5\text{Cd}_2$ : C, 40.07; H, 5.56; N, 7.79. Found: C, 40.01; H, 5.59; N, 7.75. IR (KBr,  $\text{cm}^{-1}$ ): 3495–3593(br, m), 2961(w), 1650-(vs), 1633(m), 1514(m), 1460(m), 1365(m), 1229(s), 1161(m), 1095(w), 1056(w), 1018(w), 958(w), 865(w), 743(m), 551(w). FAB-MS:  $m/z$  254 ( $[\text{H}_2\text{L}^5 + 1]^+$ , 93%). As for compound **6**, it was obtained by exposure to the air for about three days, with the departure of water molecules in crystal matrices. Orange crystals (**5**) were gradually changed into pale yellow crystals (**6**).

**Characterization data of  $[(\text{H}_2\text{L}^5)_2]^{2+} \cdot [\text{CdCl}_4]^{2-}$  (6).** Elemental analysis calcd (%) for  $\text{C}_{24}\text{H}_{38}\text{Cl}_4\text{N}_4\text{O}_4\text{Cd}_2$ : C, 41.10; H, 5.42; N, 7.99. Found: C, 41.08; H, 5.59; N, 7.91. FT-IR (KBr,  $\text{cm}^{-1}$ ): 3459–3537(br, m), 2945(m), 1653(vs), 1631(s), 1463(s), 1385(w), 1279(s), 1151(m), 1040(m), 897(w), 761(s), 641(m), 569(w), 475(w). FAB-MS:  $m/z$  254 ( $[\text{H}_2\text{L}^5 + 1]^+$ , 97%).

**Conversion among Complexes **1–5**.** When the pH of methanol solution containing single crystals of **1** (1 mmol) was adjusted to 8, after slow evaporation at room temperature for one week, pale yellow plate-like crystals of compound **2** were obtained. Similar methods were applied to the conversions of complexes **2** and **3**, at different pH = 5, similarly for **3** → **4** and pH = 3, **2** → **5**. Composition and structures of **2**, **4**, and **5** were confirmed by elemental analysis, single crystal and powder X-ray diffraction.

**DPPH Radical Scavenging Activity.** DPPH (2,2-diphenyl-1-picrylhydrazyl) radical scavenging activity was evaluated according to the method described previously.<sup>15</sup> One milliliter of every kind of ethanol extract at five concentrations (1, 0.5, 0.25, 0.125, and 0.0625 mg/mL) was mixed with 5 mL of a DPPH solution (46 mg/L) prepared daily, respectively. The mixture was mixed thoroughly and allowed to stand at room temperature in the dark for 30 min, and the absorbance of the resulting solution was measured spectrophotometrically at 517 nm. Each sample and positive control (ascorbic acid) was done in triplicate. DPPH versus using absorbance values were plotted against the percentage of DPPH (% DPPH) to estimate a 50% reduction of its initial value (IC<sub>50</sub>, oxidant index). The percent scavenging activity was calculated using the following formula:

$$\text{scavenging activity (\%)} = \frac{(\text{abs of control} - \text{abs of sample})}{\text{abs of control}} \cdot 100$$

**Crystal Structure Determination.** Data collections were performed at 298 K on a Bruker Smart Apex II diffractometer with graphite-monochromated Mo K $\alpha$  radiation ( $\lambda = 0.71073 \text{ \AA}$ ) for **1**, **3**, **4**, **5**, and **6**. Absorption corrections were applied by using the multiscan program SADABS.<sup>17</sup> Structural solutions and full-matrix least-squares refinements based on  $F^2$  were performed with the SHELXS-97<sup>18</sup> and SHELXL-97<sup>19</sup> program packages, respectively. All the non-hydrogen atoms were refined anisotropically. The hydrogen atoms were placed at calculated positions and included in the refinement in the riding model approximation. The organic

**Table 1.** Crystallographic Data for Five Compounds: **1**, **3–6**

	<b>1</b>	<b>3</b>	<b>4</b>	<b>5</b>	<b>6</b>
empirical formula	C <sub>49</sub> H <sub>74</sub> Cl <sub>8</sub> N <sub>8</sub> O <sub>10</sub> Cd <sub>6</sub>	C <sub>12</sub> H <sub>18</sub> Cl <sub>4</sub> N <sub>2</sub> O <sub>2</sub> Cd <sub>2</sub>	C <sub>16</sub> H <sub>18</sub> N <sub>6</sub> S <sub>4</sub> Cd	C <sub>24</sub> H <sub>40</sub> Cl <sub>4</sub> N <sub>4</sub> O <sub>5</sub> Cd <sub>2</sub>	C <sub>24</sub> H <sub>38</sub> Cl <sub>4</sub> N <sub>4</sub> O <sub>4</sub> Cd <sub>2</sub>
formula weight	1893.16	588.88	844.67	718.80	700.78
crystal system	triclinic	monoclinic	triclinic	orthorhombic	monoclinic
space group	<i>P</i> − <i>1</i>	<i>P</i> 2(1)/ <i>c</i>	<i>P</i> − <i>1</i>	<i>P</i> <i>bca</i>	<i>C</i> <i>c</i>
<i>a</i> [Å]	11.1490(9)	9.8814(11)	10.0956(14)	15.8574(15)	28.765(6)
<i>b</i> [Å]	14.2596(11)	10.5662(12)	10.3352(14)	18.4030(17)	10.8357(19)
<i>c</i> [Å]	21.7570(18)	18.482(2)	13.1821(18)	21.728(2)	21.467(4)
$\alpha$ [°]	94.1700(10)	90	72.2370(10)	90	90
<i>B</i> [°]	92.9330(10)	101.496(2)	74.3520(10)	90	110.063(2)
$\gamma$ [°]	90.5060(10)	90	73.6300(10)	90	90
<i>V</i> [Å <sup>3</sup> ]	3445.0(5)	1891.0(4)	1231.1(3)	6340.7(10)	6285(2)
<i>Z</i>	2	4	2	8	8
<i>T</i> [K]	298 (2)	298(2)	298(2)	298(2)	298(2)
<i>F</i> (000)	1856	1136	808	2944	2864
$\rho_{\text{calcd}}$ [g cm <sup>−3</sup> ]	1.825	2.069	2.279	1.506	1.481
$\mu$ [mm <sup>−1</sup> ]	2.183	2.819	3.348	1.064	1.069
$\lambda$ [Å]	0.71073	0.71073	0.71073	0.71073	0.71073
<i>R</i> <sub>int</sub>	0.0185	0.0576	0.0236	0.0425	0.0918
data/restraints/param	11409/3/743	3355/0/203	4419/6/275	5700/3/361	8316/2/679
GOF	1.029	1.009	1.038	1.019	1.017
<i>R</i> <sub>1</sub> [ <i>I</i> = 2 <i>σ</i> ( <i>I</i> )]	0.0374	0.0382	0.0195	0.0348	0.0596
<i>wR</i> <sub>2</sub> (all data)	0.0944	0.0626	0.0452	0.0988	0.1047

hydrogen atoms were generated geometrically (C–H = 0.93 or 0.96 Å), and the water hydrogen atoms were located from different maps and refined with isotropic temperature factors. Details of the crystal parameters, data collections, and refinements for five complexes (**1**, **3**, **4**, **5**, and **6**) are summarized in Table 1. Hydrogen-bonding data of five complexes are listed in Table S1. Further details are provided in Supporting Information.

CCDCs 766400, 766401, 766402, 766403, and 766404 are, respectively, for five complexes **1**, **3**, **4**, **5**, and **6** and contain the supplementary crystallographic data for this paper. These data can be obtained free of charge from The Cambridge Crystallographic Data Centre via [www.ccdc.cam.ac.uk/data\\_request/cif](http://www.ccdc.cam.ac.uk/data_request/cif).

**Acknowledgment.** The authors are grateful for financial aid from the National Natural Science Foundation of P. R. China (Grant No. 20772037), the Science and Technology Planning Project of Guangdong Province (Grant No. 2006A10902002), and the National Science Foundation of Guangdong Province (Grant Nos. 9251063101000006 and 06025033). P.K.T., J.L., and G.J.E. thank the U.S. Department of Energy, Office of Basic Energy Sciences, Division of Materials Sciences and Engineering under Award KC020105-FWP12152. PNNL is a multiprogram national laboratory operated for DOE by Battelle under Contract DE-AC05-76RL01830.

**Supporting Information Available:** Table of distances and angles of hydrogen bonds for **3–6**; table of fluorescence lifetimes, fluorescence quantum yields, optical density, maximum excitation wavelength, fitted value for **1–5** and ligand HL<sup>5</sup>; table of IC50 (scavenging of 50% DPPH radical) values of the methanol extracts of ligand HL<sup>5</sup> and compounds **1–5**. Figure S1: TGA curves for compounds **1–6**. Figure S2: Dimer in **1** constructed by intermolecular C–H···Cl hydrogen bonding interactions. Figure S3: Molecular structure of dinuclear compound **2** with the atom-numbering scheme. Figure S4: Packing view with 1D Δ-(right-) and Λ-(left-handed) helical methanol chains. Figure S5: 3D network in **3** constructed by π···π stacking and C–H···Cl hydrogen bonding interactions in the *ac* plane. Figure S6: 3D supramolecular in **4** constructed by O–H···O, O–H···Cl and C–H···π stacking interactions between the two adjacent two-dimensional layers in the *bc* plane. Figure S7: 3D supramolecular in **5** constructed by hydrogen bonding O–H···N, O–H···Cl and C–H···Cl interactions in the *ac* plane. Figure S8: 3D supramolecular in **6** constructed by hydrogen bonding N–H···O, O–H···N, and C–H···Cl interactions in the *ac* plane. Figure S9: The experimental and simulated PXRD patterns of complexes **1–6**. Figure S10: Scavenging activity of the methanol extracts of ligand HL<sup>5</sup> and compounds

**1–5.** This material is available free of charge via the Internet at <http://pubs.acs.org>.

## References

- (a) Ganguly, R.; Sreenivasulu, B.; Vittal, J. J. *Coord. Chem. Rev.* **2008**, *252*, 1027–1050. (b) Vigato, P. A.; Tamburini, S.; *Coord. Chem. Rev.* **2004**, *248*, 1717–2128, and references therein; (c) Casella, L.; Gullotti, M.; Pacchionic, G. *J. Am. Chem. Soc.* **1982**, *104*, 2386–2388. (d) Cui, X.-G.; Hu, Q.-P. *Chin. Chem. Lett.* **1994**, *5*, 893–896. (e) Lo, W.-K.; Wong, W.-K.; Wong, W.-Y.; Guo, J.-P. *Eur. J. Inorg. Chem.* **2005**, 3950–3954. (f) Sen, S.; Talukder, P.; Dey, S. K.; Mitra, S.; Rosair, G.; Hughes, D. L.; Yap, G. P. A.; Pilet, G.; Gramlich, V.; Matsushita, T. *Discuss. Faraday Soc.* **2006**, 1758–1765. (g) Cui, X.-G.; Hu, Q.-P.; Hu, S.-Z. *Acta Chim. Sinica* **2000**, *58*, 356–360.
- (a) Dhara, K.; Ratha, J.; Manassero, M.; Wang, X.-Y.; Gao, S.; Banerjee, P. *J. Inorg. Biochem.* **2007**, *101*, 95–103. (b) Sen, S.; Talukder, P.; Dey, S. K.; Mitra, S.; Rosair, G.; Hughes, D. L.; Yap, G. P. A.; Pilet, G.; Gramlich, V.; Matsushita, T. *J. Chem. Soc., Dalton Trans.* **2006**, 1758–1767. (c) Morris, G. A.; Zhou, H.; Stern, C. L.; Nguyen, S. T. *Inorg. Chem.* **2001**, *40*, 3222–3227. (d) Fang, H.-C.; Yi, X.-Y.; Gu, Z.-G.; Zhao, G.; Wen, Q.-Y.; Zhu, J.-Q.; Xu, A.-W.; Cai, Y.-P. *Cryst. Growth Des.* **2009**, *9*, 3776–3788. (e) Yuan, G.-Z.; Zhu, C.-F.; Xuan, W.-M.; Cui, Y. *Chem.—Eur. J.* **2009**, *15*, 6428–6434.
- (a) Shii, Y.; Motoda, Y.; Matsuo, T.; Kai, F.; Nakashima, T.; Tuchagues, J.-P.; Matsumoto, N. *Inorg. Chem.* **1999**, *38*, 3513–3522. (b) Wu, S.-T.; Long, L.-S.; Huang, L.-S.; Zheng, L. S. *Cryst. Growth Des.* **2007**, *7*, 1746–1752. (c) Mukherjee, P.; Drew, M. G. W.; Estrader, M.; Ghosh, A. *Inorg. Chem.* **2008**, *47*, 7784–7791. (d) Choudhury, S. R.; Jana, A. D.; Chen, C.-Y.; Dutta, A.; Colacio, E.; Lee, H. M.; Mostafa, G.; Mukhopadhyay, S. *CrystEngComm* **2008**, *10*, 1358–1363. (e) Sha, J.-Q.; Peng, J.; Lan, Y.-Q.; Su, Z.-M.; Pang, H.-J.; Tian, A.-X.; Zhang, P.-P.; Zhu, M. *Inorg. Chem.* **2008**, *47*, 5145–5153. (f) Reddy, L. S.; Bethune, S. J.; Kampf, J. W.; Rodriguez-Hornedo, N. *Cryst. Growth Des.* **2009**, *9*, 378–385. (g) Yu, F.; Kong, X.-J.; Zheng, Y. Y.; Ren, Y. P.; Long, L.-S.; Huang, R.-B.; Zheng, L.-S. *Dalton Transact.* **2009**, *43*, 9503–9509.
- (a) Wu, C. D.; Hu, A.; Zhang, L.; Lin, W. *J. Am. Chem. Soc.* **2005**, *127*, 8940–1. (b) Thallapally, P. K.; Tian, J.; Kishan, M. R.; Fernandez, C. A.; Dalgarno, S. J.; McGrail, P. B.; Warren, J. E.; Atwood, J. L. *J. Am. Chem. Soc.* **2008**, *130*, 16842–16843. (c) McKinlay, R. M.; Thallapally, P. K.; Atwood, J. L. *Chem. Commun.* **2006**, 2956–2958. (d) Yaghi, O. M.; O'Keeffe, M.; Ockwig, N. W.; Chae, H. K.; Eddaoudi, M.; Kim, J. *Nature* **2003**, *423*, 705–14. (e) Kitaura, R.; Seki, K.; Akiyama, G.; Kitagawa, S. *Angew. Chem., Int. Ed.* **2003**, *42*, 428–430. (f) Dalgarno, S. J.; Thallapally, P. K.; Barbour, L. J.; Atwood, J. L. *Chem. Soc. Rev.* **2007**, *36*, 236–45. (g) Ferey, G.; Mellot-Draznieks, C.; Serre, C.; Millange, F. *Acc. Chem. Res.* **2005**, *38*, 217–25. (h) Zhao, X.; Xiao, B.; Fletcher, A. J.; Thomas, K. M.; Bradshaw, D.; Rosseinsky, M. J. *Science* **2004**, *306*, 1012–1015. (i) Nouar, F.; Eubank, J. F.; Bousquet, T.; Wojtas, L.; Zaworotko, M. J.; Eddaoudi, M. *J. Am.*

- Chem. Soc.* **2008**, *130*, 1833–1835. (j) Zhao, D.; Yuan, D.; Sun, D.; Zhou, H. C. *J. Am. Chem. Soc.* **2009**, *131*, 9186–9188. (k) Ma, S. Q.; Simmons, J. M.; Yuan, D. Q.; Li, J. R.; Weng, W.; Liu, D. J.; Zhou, H. C. *Chem. Commun.* **2009**, 4049–4051. (l) McKinlay, R. M.; Thallapally, P. K.; Cave, G. W. V.; Atwood, J. L. *Angew. Chem., Int. Ed.* **2005**, *44*, 5733–5736.
- (5) (a) Thallapally, P. K.; McGrail, P. B.; Dalgarno, S. J.; Atwood, J. L. *Cryst. Growth Des.* **2008**, *8*, 2090–2092. (b) Thallapally, P. K.; McGrail, B. P.; Dalgarno, S. J.; Schaeff, H. T.; Tian, J.; Atwood, J. L. *Nat. Mater.* **2008**, *7*, 146–150. (c) Thallapally, P. K.; Tian, J.; Motkuri, R. K.; Fernandez, C. A.; Dalgarno, S. J.; McGrail, P. B.; Warren, J. A.; Atwood, J. L. *J. Am. Chem. Soc.* **2008**, *130*, 16842.
- (6) (a) Battistuzzi, G.; Borsari, M.; Menabue, L.; Saladini, M.; Sola, M. *Inorg. Chem.* **1996**, *35*, 4239–4247. (b) Dalgarno, S. J.; Hardie, M. J.; Raston, C. L. *Cryst. Growth Des.* **2004**, *4*, 227–234. (c) Zhou, Z.-H.; Deng, Y.-F.; Wan, H.-L. *Cryst. Growth Des.* **2005**, *5*, 1109–1117. (d) Go, Y. B.; Wang, X.; Anokhina, E. V.; Jacobson, A. J. *Inorg. Chem.* **2005**, *44*, 8265–8271. (e) Zheng, P.-Q.; Ren, Y.-P.; Long, L.-S.; Huang, R.-B.; Zheng, L.-S. *Inorg. Chem.* **2005**, *44*, 1190–1192. (f) Zhang, G. Q.; Yang, G. Q.; Ma, J. S. *Cryst. Growth Des.* **2006**, *6*, 375–381. (g) Lu, W.-G.; Jiang, L.; Feng, X.-L.; Lu, T.-B. *Cryst. Growth Des.* **2006**, *6*, 564–571.
- (7) Zhou, X.-X.; Cai, Y.-P.; Zhu, S.-Z.; Zhan, Q.-G.; Liu, M.-S.; Zhou, Z.-Y.; Chen, L. *Cryst. Growth Des.* **2008**, *8*, 2076–2080.
- (8) Fang, H.-C., Ge, Y.-Y., Zheng, S.-R., Zhan, Q.-G., Zhou, Z.-Y., Chen, L., Ying, Y., Cai, Y.-P. *Cryst. Growth Des.* **2010**, in press.
- (9) (a) Shen, Y.-L.; Mao, J. G. *Inorg. Chem.* **2005**, *44*, 5328–5335. (b) Li, H.-X.; Ren, Z. G.; Zhang, Y.; Zhang, W. H.; Lang, J. P.; Shen, Q. *J. Am. Chem. Soc.* **2005**, *127*, 1122–1123.
- (10) (a) Lu, J. J.; Kochi, J. K. *Cryst. Growth Des.* **2009**, *9*, 291–296. (b) Goodgame, D. M. L.; Kealey, S.; Lickiss, P. D.; White, A. J. P. *J. Mol. Struct.* **2008**, *890*, 232–239. (c) Kong, L.-Y.; Lu, X.-H.; Huang, Y.-Q.; Kawaguchi, H.; Chu, Q.; Zhu, H. F.; Sun, W. Y. *J. Solid State Chem.* **2007**, *180*, 331–338.
- (11) (a) Thallapally, P. K.; Nangia, A. *CrystEngComm* **2001**, *27*, 114. (b) Desiraju, G. R. *Angew. Chem.* **1995**, *107*, 2541–2558. (c) Thallapally, P. K.; Katz, A. K.; Carrell, H. L.; Desiraju, G. R. *Chem. Commun.* **2002**, 344–345.
- (12) Wang, X. L.; Qin, C.; Wang, E. B.; Xu, L.; Su, Z. M.; Hu, C. W. *Angew. Chem. Int. Ed.* **2004**, *43*, 5036–5040.
- (13) Xu, J.-G.; Wang, Z.-B. *Fluorescence Analytical Methods*, 3rd ed.; Chinese Science Publishing Company, 2006.
- (14) Majumder, A.; Rosair, G. M.; Mallick, A.; Chattopadhyay, N.; Mitra, S. *Polyhedron* **2006**, *25*, 1753–1762.
- (15) (a) Lin, J.-X.; Lin, M.-L.; Su, Y.-J.; Liu, M.-S.; Cai, Y.-P. *Trans. Metal Chem.* **2007**, *32*, 338343. (b) Hong, S.-F.; Liang, X.-H.; Fang, H.-C.; Zhou, Z.-Y.; Hu, Z.-J.; Cai, Y.-P. *Trans. Metal Chem.* **2009**, *34*, 115–120.
- (16) (a) Peng, C.-L.; Chen, S.-W.; Lin, Z.-F. *Prog. Biochem. Biophys.* **2000**, *27*, 658–661. (b) Chun, S.-S.; Vattet, D.-A.; Lin, Y.-T. *Process Biochem.* **2005**, *40*, 809–816. (c) González, A.; Gómez, E.; Cortés-Lozada, A.; Hernández, S.; Ramírez-Apan, T.; Nieto-Camaceo, A. *Chem. Pharm. Bull.* **2009**, *57*, 5–15. (d) Rekha, M. N.; Yadav, A. R.; Dharmesh, S.; Chauhan, A. S.; Ramteke, R. S. *Food Bioprocess Technol.* **2008**, *10*, 1947–1956.
- (17) Sheldrick, G. M. *SADABS*, version 2.05; University of Göttingen: Göttingen, Germany.
- (18) Sheldrick, G. M. *SHELXS-97, Program for X-ray Crystal Structure Determination*; University of Göttingen: Göttingen, Germany, 1997.
- (19) Sheldrick, G. M. *SHELXS-97, Program for X-ray Crystal Structure Refinement*; University of Göttingen: Göttingen, Germany, 1997.